Diffractive J/ψ photoproduction in a dual model

R. Fiore,[1] L. L. Jenkovszky,[2] V. K. Magas,[3] F. Paccanoni,[4] and A. Prokudin[5]

[1]*Universita' della Calabria, Dipartimento di Fisica Arcavacata di Rende, I-87030 Cosenza, Calabria, Italy*
[2]*Bogolyubov Institute for Theoretical Physics (BITP), Ukrainian National Academy of Sciences,
14-b, Metrolohichna street, Kiev, 03143, Ukraine*
[3]*Departament d'Estructura i Constituents de la Matéria, Universitat de Barcelona, Diagonal 647, 08028 Barcelona, Spain*
[4]*Universita' di Padova, Dipartimento di Fisica and INFN, sezione di Padova, via Marzolo 8, I-35100 Padua, Italy*
[5]*Dipartimento di Fisica Teorica, Università di Torino and INFN, Sezione di Torino, via P. Giuria 1, I-10125 Torino, Italy*

J/ψ photoproduction is studied in the framework of the analytic *S*-matrix theory. The differential and integrated elastic cross sections for J/ψ photoproduction are calculated from a dual amplitude with Mandelstam analyticity. It is argued that, at low energies, the background, which is the low-energy equivalent of the high-energy diffraction, replaces the Pomeron exchange. The onset of the high-energy Pomeron dominance is estimated from the fits to the data.

I. INTRODUCTION

J/ψ photoproduction is a unique testing field for diffraction. Most of the theoretical approaches to J/ψ photoproduction are based on the Pomeron or multigluon exchanges in the *t* channel of the reaction (for a review see [1]). A common feature of these models is the uncertainty of the low-energy extrapolation of the high-energy exchange mechanisms. The missing piece is the low-energy background contribution, significant between the threshold and the region of the dominance of the exchange mechanism, e.g., the onset of the Regge-Pomeron asymptotic behavior.

What is the fate of the Regge exchange contribution when extrapolated to low energies? The answer to this question was given in the late 1960s by dual models: the proper sum of direct-channel resonances produces Regge asymptotic behavior and vice versa. The alternative, i.e. taking the sum of the two (the so-called interference model), is incorrect, resulting in double counting.

While the realization of the Regge-resonance duality was quantified within narrow-resonance dual models, notably in the Veneziano model [2], a similar solution for the Pomeron (= diffraction) was not possible in the framework of that model, just because of its narrow-resonance nature. Another reason for the poor understanding of "low-energy diffraction," or the background, is difficulties in its separation (discrimination and identification), because of the mixing with the resonance part.

Experimentally, the identification of these two components meets difficulties coming from the flexibility of their parametrizations. The separation of a Breit-Wigner resonance from the background, as well as the discrimination of some *t*-channel exchanges with identical flavor content and *C* parity, e.g. the Pomeron mixing with the *f* meson or the odderon with ω, is a familiar problem in experimental physics.

Now we have an ideal opportunity in hand: J/ψ photoproduction is purely diffractive since resonances here are not produced and, due to the Okubo-Zweig-Iizuka (OZI) rule [3], no flavor (valence quarks) can be exchanged in the *t* channel. The derivation of the OZI rule is based on simple quark diagrams and they are closely related to the so-called duality quark diagrams, to be discussed in the next section.

In the next section we shortly remind the reader about the basics of the two-component duality. In Sec. III a dual model applicable to both the diffractive and nondiffractive (resonance) components of the amplitude is introduced. Its application to J/ψ photoproduction is presented in Sec. IV. The onset of the Regge asymptotic behavior is shown in Sec. V, where various Pomeron trajectories are confronted. A short summary of the paper is given in Sec. VI.

II. TWO-COMPONENT DUALITY

According to our present knowledge about two-body hadronic reactions, two distinct classes of reaction mechanisms exist.

The first one includes the formation of resonances in the *s* channel and the exchange of particles, resonances, or Regge trajectories in the *t* channel. The low-energy resonance behavior and the high-energy Regge asymptotics are related by duality, illustrated in Fig. 1(a), which at Born level, or, alternatively, for tree diagrams, mathematically can be formalized in the Veneziano model, which is a combination of Euler Beta functions [2].

The second class of mechanisms does not exhibit resonances at low energies and its high-energy behavior is governed by the exchange of a vacuum Regge trajectory, the Pomeron, with an intercept equal to or slightly greater than 1. Harari and Rosner [4] hypothesized that the low-energy nonresonating background is dual to the high-energy Pomeron exchange, or diffraction. In other words, the low-energy background should extrapolate to high-energy diffraction in the same way as the sum of narrow
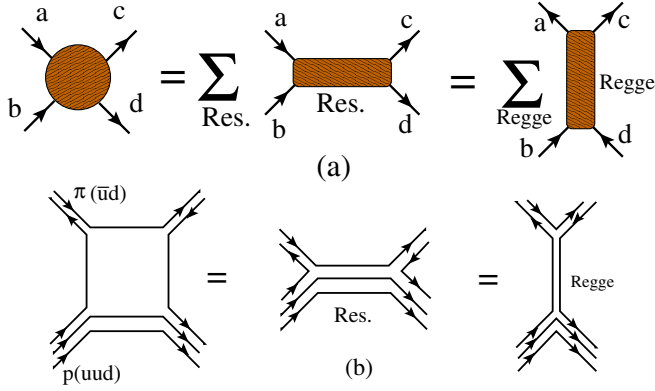
FIG. 1 (color online).   (a) By duality, the proper sum of resonances in the direct channel produces its asymptotic Regge behavior and vice versa; (b) the same equality in terms of duality quark diagrams.
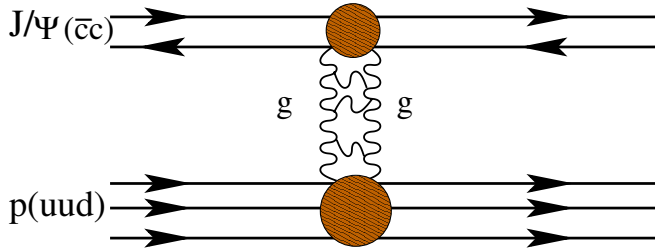

FIG. 2 (color online).   Duality quark diagram for elastic J/ψ-p scattering.

resonances produces Regge behavior. However, contrary to the case of narrow resonances, the Veneziano amplitude, by construction, cannot be applied to (infinitely) broad resonances. This becomes possible in a generalization of narrow-resonance dual models called dual amplitudes with Mandelstam analyticity (DAMA), allowing for (infinitely) broad resonances [5], or the background.

Duality has an elegant interpretation in terms of quark-partons, called dual quark diagrams (Figs. 1 and 2). Theses diagrams can be deformed by conserving their topology as shown in Fig. 1(b), where direct-channel resonances correspond to the quark box squeezed in the horizontal direction and Regge exchange corresponds to squeezing it vertically.

Resonances can be formed only in nonexotic channels, made of a quark and antiquark pair (meson) or three quarks (baryon), as e.g. in the $\pi^- p$ channel, shown in Fig. 1(b).

Resonances cannot be produced in exotic channels, e.g. in proton-proton scattering (a two-baryon state) or in $K^+ p$ scattering, while $p\bar{p}$ and $K^- p$ are nonexotic and exhibit observable resonances. According to the two-component duality hypotheses [4], the nonresonating direct-channel background is dual to a Pomeron exchange. By drawing a duality quark diagram, it is easy to see that, by the OZI rule, a quark-antiquark pair cannot be exchanged in the t channel of an exotic reaction. The interaction can be mediated by multigluon (Pomeron) exchange, as illustrated in Fig. 2 for J/ψ-p scattering.

The above simple rules are confirmed experimentally: total cross section of pp and $K^- p$ scattering exhibits a rich resonance structure (nonexotic channels) and a rapid decrease at high energies due to the decreasing contribution from subleading Reggeons, while $p\bar{p}$ and $K^+ p$ total cross sections are nearly flat due to the nonresonant low-energy background, dual to the high-energy Pomeron exchange—both being of diffractive nature. The above rules are not exact due to the presence of mixed states, violation of exchange degeneracy of t channel trajectories, unitarity corrections (nonplanar diagrams), etc. These effects are less important in J/ψ-p scattering.

The two-component dual picture of hadronic dynamics is summarized in Table I.

III. DUAL MODEL

Dual models with Mandelstam analyticity [6] appeared as a generalization of narrow-resonance (e.g. Veneziano) dual models, intended to overcome the manifestly nonunitarity of the latter. Contrary to narrow-resonance dual models, DAMA requires nonlinear, complex trajectories. This property allows for the presence in DAMA of finite-width resonances and a nonvanishing imaginary part of the amplitude. The maximal number of direct resonances is correlated with the maximal value of the real part of the relevant trajectory or, alternatively, with the mass of its heaviest threshold. An extreme case is when the real part of the trajectory terminates below the spin of the lowest (s-channel) resonance, called ''super-broad-resonance approximation'' [5], in contrast with the narrow-resonance approximation, e.g., of the Veneziano amplitude. The resulting scattering amplitude can describe the nonresonating direct-channel background, dual to the Pomeron exchange in the t channel. The dual properties of this construction were studied in Ref. [7].

TABLE I.   Two-component duality.

Im$A(a + b \rightarrow c + d) =$	R	Pomeron
s channel	$\sum A_{\text{Res}}$	Nonresonant background
t channel	$\sum A_{\text{Regge}}$	Pomeron ($I = S = B = 0$; $C = +1$)
Duality quark diagram	Fig. 1(b)	Fig. 2
High-energy dependence	$s^{\alpha-1}$, $\alpha < 1$	$s^{\alpha-1}$, $\alpha \geq 1$

The (s, t) term (s and t are Mandelstam variables) of a DAMA [6] is given by

$$D(s, t) = c \int_0^1 dz \left(\frac{z}{g}\right)^{-\alpha(s')-1} \left(\frac{1-z}{g}\right)^{-\alpha_t(t')}, \quad (1)$$

where $\alpha(s)$ and $\alpha(t)$ are Regge trajectories in the s and t channels, correspondingly; $s' = s(1 - z)$, $t' = tz$; g and c are parameters, $g > 1$, $c > 0$.

For $s \to \infty$ and fixed t DAMA, Eq. (1), is Regge behaved

$$D(s, t) \sim s^{\alpha_t(t)-1}. \quad (2)$$

In the vicinity of the threshold, $s \to s_0$,

$$D(s, t) \sim \sqrt{s_0 - s}[\text{const} + \ln(1 - s_0/s)]. \quad (3)$$

The pole structure of DAMA is similar to that of the Veneziano model except that multiple poles appear on daughter levels [6].

$$D(s, t) = \sum_{n=0}^{\infty} g^{n+1} \sum_{l=0}^{n} \frac{[-s\alpha'(s)]^l C_{n-l}(t)}{[n - \alpha(s)]^{l+1}}, \quad (4)$$

where $C_n(t)$ is the residue, whose form is fixed by the t-channel Regge trajectory (see [6])

$$C_l(t) = \frac{1}{l!} \frac{d^l}{dz^l} \left[\left(\frac{1-z}{g}\right)^{-\alpha_t(tz)}\right]_{z=0}. \quad (5)$$

The pole term in DAMA is a generalization of the Breit-Wigner formula, comprising a whole sequence of resonances lying on a complex trajectory $\alpha(s)$. Such a "Reggeized" Breit-Wigner formula has little practical use in the case of linear trajectories, resulting in an infinite sequence of poles, but it becomes a powerful tool if complex trajectories with a limited real part and hence a restricted number of resonances are used.

A simple model of trajectories satisfying the threshold and asymptotic constraints is a sum of square roots [6]

$$\alpha(s) \sim \sum_i \gamma_i \sqrt{s_i - s}. \quad (6)$$

The number of thresholds included depends on the model. While the lightest threshold gives the main contribution to the imaginary part, the heaviest one promotes the rise of the real part (terminating at the heaviest threshold).

A particular case of the model equation (6) is that with a single threshold,

$$\alpha(s) = \alpha(0) + \alpha_1(\sqrt{s_0} - \sqrt{s_0 - s}). \quad (7)$$

Imposing an upper bound on the real part of this trajectory, $\text{Re}\alpha(s) < 0$, we get an amplitude that does not produce resonances, since the real part of the trajectory does not reach $n = 0$ where the first pole could appear. This is the ansatz we suggest for the exotic trajectory. The imaginary part of such a trajectory instead rises indefinitely, contributing to the total cross section with a smooth background.

The super-broad-resonance approximation [5], in a sense, is opposite to the narrow-resonance approximation, typical of the Veneziano model. However, contrary to the latter, the superbroad resonance approximation allows for a smooth transition to observable resonances or to the "Veneziano limit" [6]. Dual properties of this model were studied in [7].

IV. J/ψ PHOTOPRODUCTION

Photoproduction of vector mesons is well described in the framework of the vector meson dominance (VMD) model [8], according to which the photoproduction scattering amplitude A is proportional to the sum of the relevant hadronic amplitudes [9] (see also [10]):

$$D_H(\gamma P \to VP) = \sum_V \frac{e}{f_V} D_H(VP \to VP), \quad (8)$$

where e is the vector meson-photon coupling constant, $V = \rho, \omega, \phi, J/\psi, \ldots$. Within this approximation, photoproduction is reduced to elastic hadron scattering (J/ψ-p in our case), where the constants e and f_V are absorbed by the normalization factor, to be fitted to the data.

Let us note that VMD at low energies, especially near the threshold where the photoproduction cross section should recover from the vanishing mass of the real photon to the finite mass of the vector meson, is only approximate. Nevertheless, the calculations presented in the next section show good agreement with the data starting from the threshold value. This may be attributed to the particular kinematics typical of DAMA, see Eq. (12) in the next section.

Among various vector mesons we choose one, namely, J/ψ, since, by the OZI rule [3], in J/ψ-p scattering only the Pomeron trajectory can be exchanged in the t channel. To a lesser extent, this is true also for the $\phi - p$ scattering; however, in the latter case, ordinary meson exchange is present due to $\omega - \phi$ mixing. Heavier vector mesons are as good as J/ψ-p, but relevant data are less abundant. So, we find J/ψ-p scattering to be an ideal testing field (filter) for diffraction: in the direct channel only exotic trajectories are allowed and they are dual to the exchange of the Pomeron trajectory. Diffraction can be studied uncontaminated by secondary trajectories. This possibility was already emphasized in earlier publications (see [5,6,11]), however without fits to the experimental data.

In the present paper we apply DAMA for meson-baryon scattering [12] with an exotic trajectory in the direct channel and the Pomeron trajectory in the exchange channel and calculate the differential and integrated elastic cross section for J/ψ-p photoproduction. The parameters of the model are fitted to the experimental data on J/ψ photoproduction. With these parameters we also calculate the imaginary part of the forward amplitude proportional to the J/ψ-p total cross section.

In the framework of the Regge-pole models, J/ψ photoproduction was studied in numerous papers. Apart from the flexibility inherent in the Regge-pole approach, there is an ambiguity in the low-energy behavior, below the Regge asymptotics. Usually, this low-energy domain is either ignored by a lower bound in the applications, or it is accounted for by the inclusion of a threshold factor. While in the first case one eliminates part of the dynamics, below the (assumed) Regge asymptotic behavior, the second option ignores the domain between the threshold and Regge asymptotic behavior, characterized by resonances in nondiffractive processes, otherwise mimicked by a direct-channel exotic contribution.

Following [13], we write the meson-baryon elastic scattering amplitude (with J/ψ photoproduction in mind) as a combination,

$$D(s, t, u) = (s - u)(D(s, t) - D(u, t)). \qquad (9)$$

For the exotic Regge trajectory such as (7) the scattering amplitude is given by a convergent integral, Eq. (9) with (1), and can be calculated for any s and t without analytical continuation, needed otherwise, as discussed in [6].

We use a t-channel Pomeron trajectory in the form

$$\alpha^P(t) = \alpha^P(0) + \alpha_1^P(\sqrt{t_1} - \sqrt{t_1 - t}) \\ + 2\alpha_2^P(t_2 - \sqrt{(t_2 - t)t_2}) \qquad (10)$$

with a light (lowest) threshold $t_1 = 4m_\pi^2$ and a heavy one t_2, whose value, together with other parameters appearing in (1), will be fitted to the data (see Table I). Equation (10) is a generalization of the trajectory with one square root threshold used in [14]. Throughout this paper $\alpha(t)$ and $\alpha^P(t)$ are identical since in the t channel only the Pomeron trajectory contributes.

Arguments from the fits in favor of a nonlinear trajectory can be found also in Ref. [16] as well as in Regge-pole models [14,15,17] fitting high-energy J/ψ photoproduction and electroproduction. The behavior of these trajectories has much in common at small $|t|$ (below, say, 2 GeV^2), whereafter they may strongly deviate. In Sec. VI we compare their behavior and add more comments on that.

The direct-channel exotic trajectory is (see [11])

$$\alpha^E(s) = \alpha^E(0) + \alpha_1^E(\sqrt{s_0} - \sqrt{s_0 - s}). \qquad (11)$$

The relevant threshold value is $s_0 = (m_{J/\psi} + m_P)^2$.

Let us remember also that s, t, and u are not independent variables but they are related by $s + t + u = \sum_i m_i^2 = 2m_{J/\psi}^2 + 2m_P^2$.

The integral of Eqs. (1) and (9):

$$D(s, t, u) = c(s - u) \int_0^1 dz \left(\frac{1 - z}{g}\right)^{-\alpha_t(t')} \left(\left(\frac{z}{g}\right)^{-\alpha(s')-1} \\ - \left(\frac{z}{g}\right)^{-\alpha(u')-1}\right), \qquad (12)$$

with exotic trajectory (11), converges for any values of s and t [18]. So, the procedure of the analytic continuation introduced in Ref. [6] and inevitable in the case of resonances can be avoided here, enabling numerical calculations with any desired precision [19].

V. DIFFERENTIAL AND INTEGRATED ELASTIC CROSS SECTION

To calculate the differential cross section we use the following normalization:

$$\frac{d\sigma}{dt} = \frac{1}{16\pi\lambda(s, m_{J/\psi}, m_P)} |D(s, t, u)|^2, \qquad (13)$$

where $\lambda(x, y, z) = x^2 + y^2 + z^2 - 2xy - 2yz - 2xz$.

The integrated elastic cross section is defined as

$$\sigma_{el}(s) = \int_{-t_{max}=s/2}^{t_{thr.}\approx 0} dt \frac{d\sigma}{dt}. \qquad (14)$$

We have fitted the parameters of the model to the data [21,22] on the J/ψ photoproduction differential cross section in the energy range W between 35 and 260 GeV. The results of the fits together with the data are shown in Fig. 4 and in the right panel of Fig. 3. The values of the fitted parameters are quoted in Table II. With these parameters we have also plotted the differential cross section at lower energies (left panel of Fig. 3). It is interesting to note that the shape of the cone (exponential decrease in t), an important characteristics of diffraction, survives at low energies.

From the fits to the differential cross section, the integrated elastic cross section was calculated, as shown in Fig. 5. The calculated curve is fully consistent with the data in the whole kinematical region. Enlarged is shown the energy region close to the threshold, where the background contribution dominates.

The aim of this fit was to demonstrate the viability of the model covering the whole kinematical region—from the threshold to highest energies and for all experimentally measured momenta transfers. Yet, it includes the important region of ''low-energy'' diffraction, located between the threshold and Regge asymptotics and described by a direct-channel exotic trajectory.
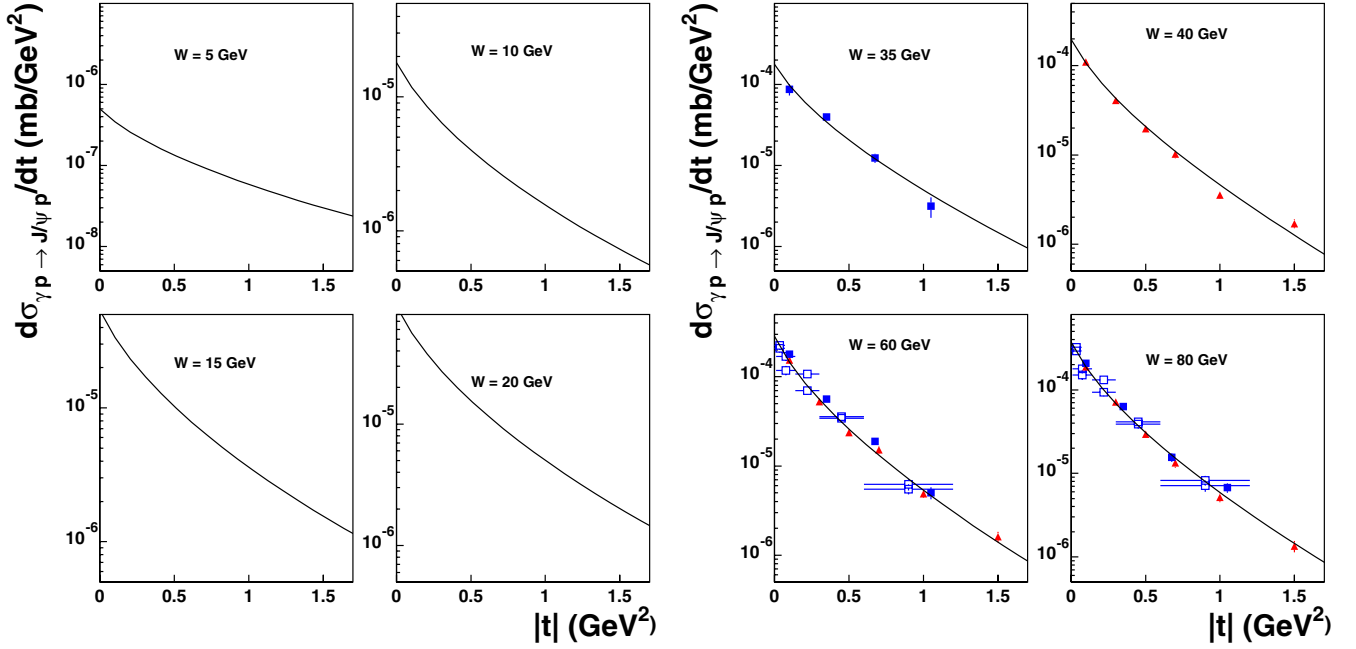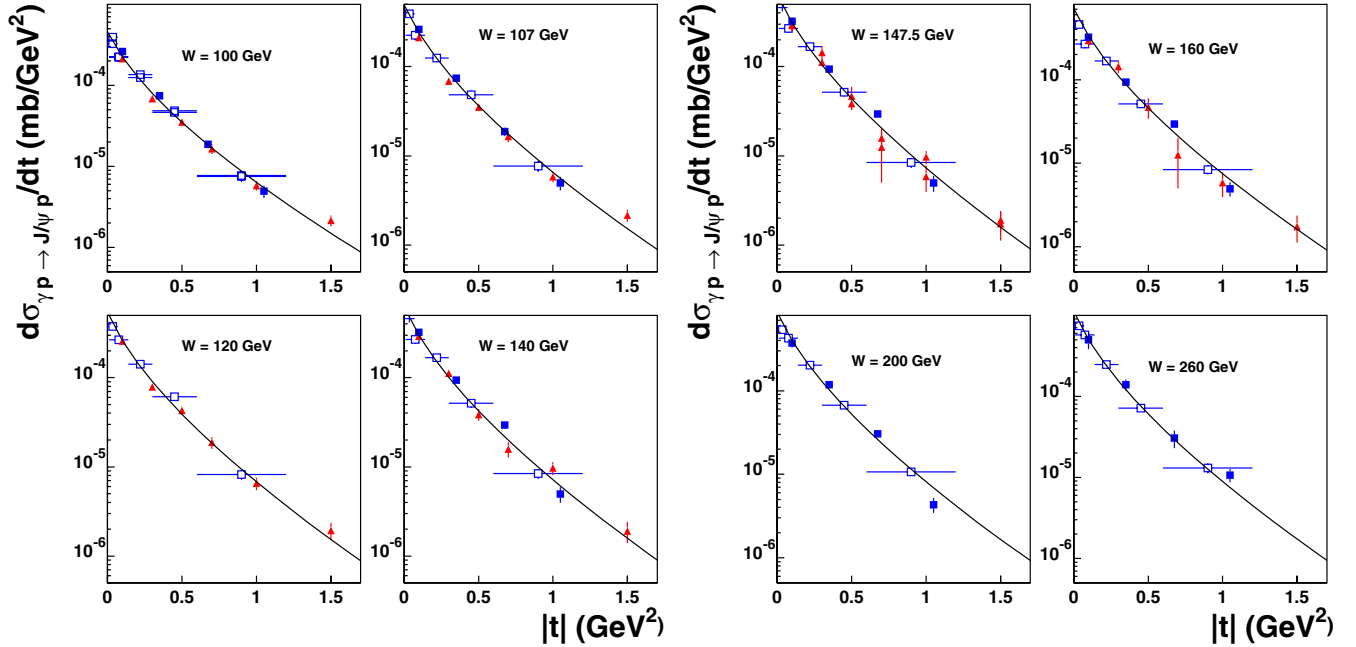
FIG. 3 (color online). J/ψ differential cross sections as a function of t in the energy range W between 5 and 80 GeV.

FIG. 4 (color online). J/ψ differential cross sections as a function of t in the range of energy W from 100 to 260 GeV.

TABLE II. Fitted values of the adjustable parameters.

$\alpha^E(0) = -1.83$	$\alpha^E_1(0) = 0.01\ (\text{GeV}^{-1})$
$\alpha^P(0) = 1.2313$	$\alpha^P_1(0) = 0.134\,98\ (\text{GeV}^{-1})$
$\alpha^P_2(0) = 0.04\ (\text{GeV}^{-2})$	$t_2 = 36\ (\text{GeV}^2)$
$g = 13\,629$	$c = 0.0025$
$\chi^2/\text{d.o.f.} = 0.83$	

VI. REGGE ASYMPTOTIC BEHAVIOR AND THE POMERON TRAJECTORY

The high-energy behavior of the dual amplitude is of Regge form, by definition. Below we scrutinize the approach to the Regge asymptotic behavior. The energy, at which the deviations from Regge behavior become relevant, can be extracted e.g. from the total cross section calculated from DAMA (with the parameters fitted to the
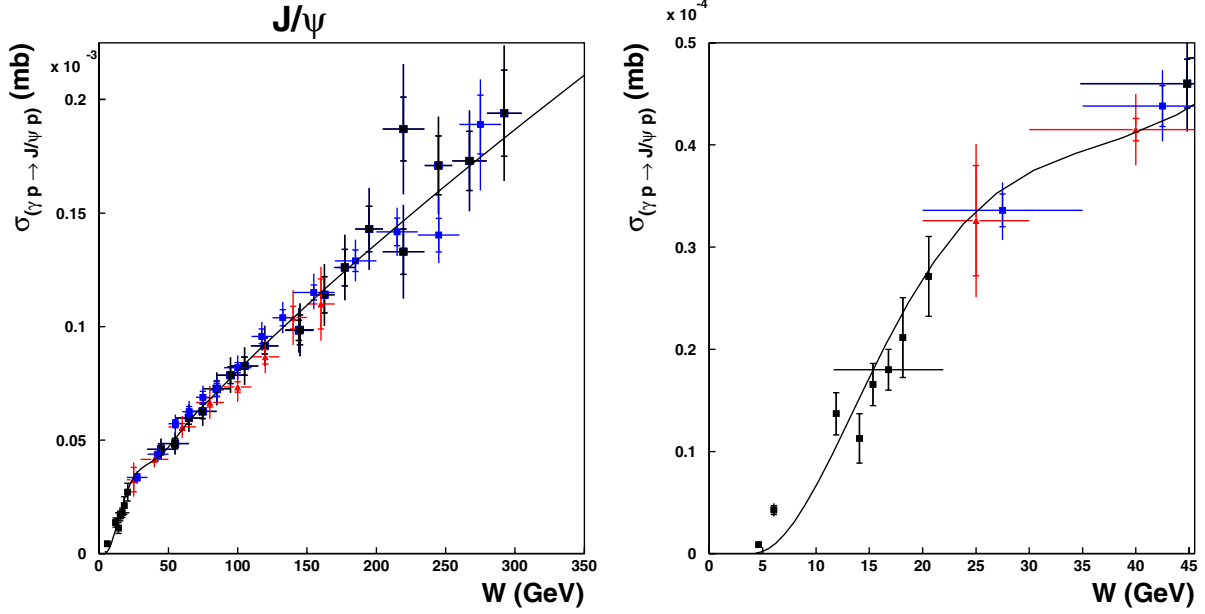
FIG. 5 (color online). J/ψ elastic cross section for all energies (left panel) and close to the threshold region (right panel).

data) divided by its asymptotic form $s^{\alpha^P(0)-1}$, as shown in Fig. 6. One can see that the ratio starts to deviate from 1 around 50 GeV, which means that, below this energy down to the threshold, nonasymptotic, non-Regge effects become important; the contribution of the background is not negligible anymore.

Beyond 50 GeV DAMA is typically Regge behaved. The remaining details affecting the Regge behavior are as follows: the form of the Regge singularity (here, a simple Regge pole) and the form of the Pomeron trajectory.

In the present paper, to fit the rise of the cross sections with energy, we used a "supercritical" Pomeron trajectory,
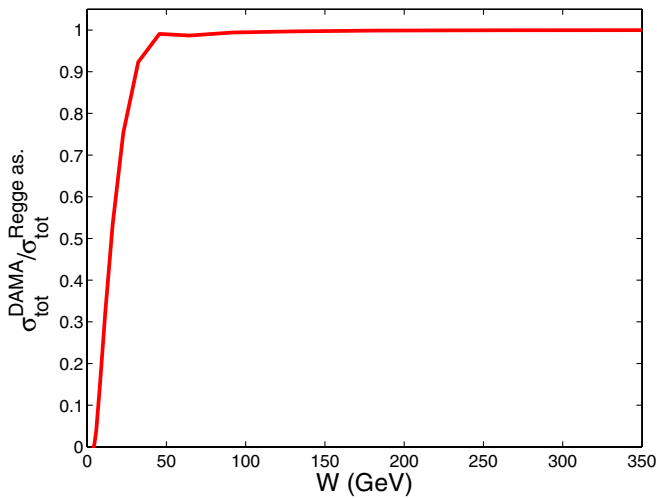
with $\alpha(0) = 1.2313$ (see Table I). Alternatively, in a dipole Pomeron model [14,15,17] cross sections rise with energy logarithmically. In other words, various versions and fits of Regge-type models give different Pomeron trajectories, as shown in Fig. 7.

Figure 7 shows, apart from our trajectory (10) with the parameters presented in Table I,

(1) the simplest linear trajectory [15], denoted in Fig. 7 as "linear":

$$\alpha^P(t) = 1.0 + 0.25 \text{ GeV}^{-2} t; \qquad (15)$$

(2) the trajectory of Ref. [16] containing a quadratic term (denoted "quadratic"):

$$\alpha^P(t) = 1.1 + 0.25 \text{ GeV}^{-2} t + 0.078 \text{ GeV}^{-4} t^2; \qquad (16)$$

(3) the trajectory with one square root threshold [14], denoted as "square root":

$$\alpha^P(t) = 1.0 + 0.138 \text{ GeV}^{-1} (\sqrt{t_1} - \sqrt{t_1 - t}),$$
$$t_1 = 4m_\pi^2. \qquad (17)$$

Although, as can be seen in Fig. 7, the intercepts of these trajectories are quite different (depending on the type of the Pomeron singularity), their slopes at small $|t|$ are nearly the same. The quadratic term in the Pomeron trajectory of [16] (chain lines in Fig. 7) rises dramatically, thus limiting its applicability to small values of $|t|$ (actually, it was fitted to the data at $|t| \leq 2$ GeV).

FIG. 6 (color online). J/ψ total cross sections versus its Regge asymptotics $\sigma_{\text{tot}}^{\text{Regge as.}} \sim s^{\alpha^P(0)-1}$. Pure Regge asymptotic behavior fails from 50 GeV downwards.
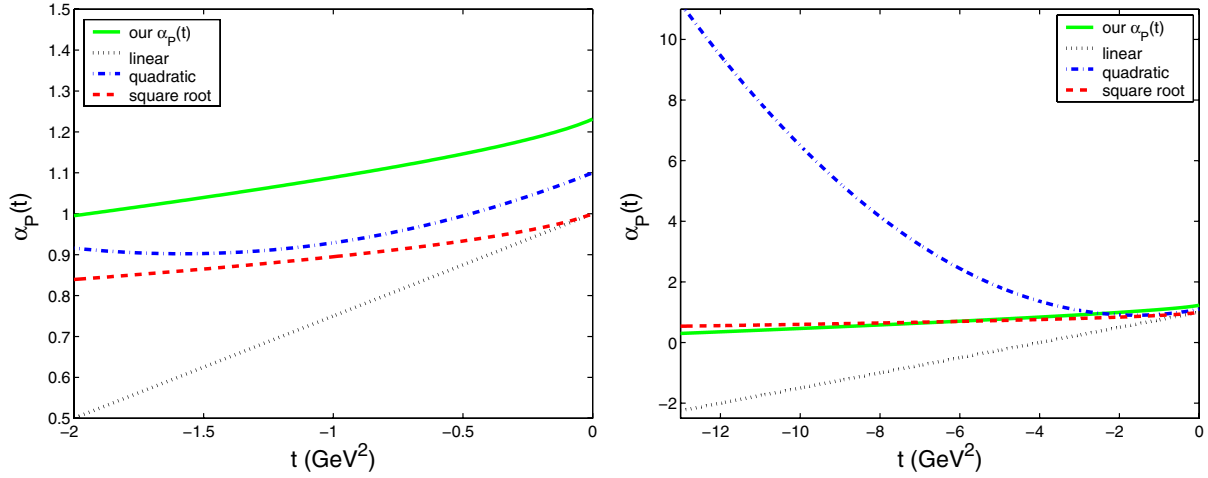
FIG. 7 (color online).   Pomeron trajectories used in Refs. [14–17]; see text.

The large-$|t|$ behavior of the nonlinear trajectories is an interesting problem by itself. As is well known, wide-angle scaling behavior of the amplitude requires a logarithmic asymptotic behavior of the trajectory. More details on this interesting subject can be found in a recent paper [23] and references therein.

VII. CONCLUSION

The low-energy part of the present model can serve as a background both in theoretical and experimental studies. We know from high-energy diffraction (= Pomeron) that it is universal. From the duality arguments one would assume that the same is true for the background, dual to the Pomeron. However, the present model of the background contains a reaction-dependent parameter, namely, the value of the direct-channel threshold mass violating this universality. To see the role of the background separately, more fits to other reactions will be necessary.

In any case, the model presented in this paper offers a complementary approach to soft dynamics of strong interactions, namely, to its component dominated by diffraction, which is beyond the scope of perturbative quantum chromodynamics.

An important finding of the present paper is the behavior of the differential cross sections at low energies, calculated with the parameters fitted to high-energy data and presented in the left panel of Fig. 3. It shows the existence of a shrinking forward cone, typical of diffraction, persist-

ing to lowest energies, dominated by the background (cf. Fig. 6).

The proper parametrization of the background is important for most of the reactions, such as pp, $p\bar{p}$, or πp scattering, and thus the obtained results are universal, and the calculated background can and should be included in any model or data analyses at low energies.

In this paper we have used the simple version of DAMA. The model can be extended to include, for example, a dipole Pomeron, which can be generated by differentiating Eq. (1) in $\alpha(t)$, as was done, e.g., in Ref. [14,15].

Generalizations to nonzero Q^2 (electroproduction) of Regge-pole models can be found in Refs. [14,15,17,23], and those of DAMA were studied in [24,25]. It should be noted however that at high Q^2 VMD may not be valid anymore. The ambitious program of a unified description of soft and hard dynamics, however, is beyond the scope of the present paper.

ACKNOWLEDGMENTS

[1] I. Ivanov, N. Nikolaev, and A. Savin, Phys. Part. Nucl. **37,** 1 (2006).

[2] G. Veneziano, Nuovo Cimento A **57,** 190 (1968).

[3] S. Okubo, Phys. Lett. **5,** 165 (1963); G. Zweig, CERN Report No. 401, 402, 412, 1964; J. Iizuka, Prog. Theor. Phys. Suppl. **37-38,** 21 (1966).

[4] H. Harari, Phys. Rev. Lett. **22**, 562 (1969); J. Rosner, Phys. Rev. Lett. **22**, 689 (1969).

[5] A. I. Bugrij, L. L. Jenkovszky, and N. A. Kobylinsky, Lett. Nuovo Cimento **5**, 389 (1972).

[6] A. I. Bugrij *et al.*, Fortschr. Phys. **21**, 427 (1973).

[7] L. L. Enkovski, Yad. Fiz. **21**, 213 (1974) [Sov. J. Nucl. Phys. **21**, 213 (1974)].

[8] J. J. Sakurai, Ann. Phys. (Paris) **11**, 1 (1960); *Currents and Mesons* (University of Chicago Press, Chicago, 1969); J. J. Sakurai and D. Schildknecht, Phys. Lett. **40B**, 121 (1972); J. Alwall and G. Ingelman, arXiv:hep-ph/0310233; for a recent review see D. Schildknecht, Acta Phys. Pol. B **37**, 595 (2006).

[9] P. D. B. Collins, *An Introduction to Regge Theory and High Energy Physics* (Cambridge University Press, Cambridge, England, 1977).

[10] L. L. Jenkovszky, E. S. Martynov, and F. Paccanoni, in *HADRONS-96, Novy Svet, 1996*, edited by G. V. Bugrij, L. L. Jenkovszky, and E. S. Martynov (BITP, Kiev, 1996), p. 170; A. Afanasev, C. E. Carlson, and C. Wahlquist, Phys. Rev. D **61**, 034014 (2000).

[11] L. L. Jenkovszky, S. Yu. Kononenko, and V. K. Magas, arXiv:hep-ph/0211158.

[12] By having accepted vector dominance, we thus reduce J/ϕ photoproduction to J/ψ-p scattering.

[13] L. L. Jenkovszky, N. A. Kobylinsky, and A. B. Prognimak, Ann. Phys. (Berlin) **32**, 81 (1975).

[14] R. Fiore, L. L. Jenkovszky, F. Paccanoni, and A. Papa, Phys. Rev. D **65**, 077505 (2002), and references therein.

[15] R. Fiore, L. Jenkovszky, and F. Paccanoni, Eur. Phys. J. C **10**, 461 (1999);

[16] A. Brandt *et al.*, Nucl. Phys. **B514**, 3 (1998).

[17] E. S. Martynov, A. Prokudin, and E. Predazzi, Eur. Phys. J. C **26**, 271 (2002); A. Prokudin, E. S. Martynov, and E. Predazzi, arXiv:hep-ph/0211430.

[18] Note that for $D(s, t)$ and $D(u, t)$, taken separately, only the imaginary parts are convergent, while their real parts diverge. However, for their difference, Eq. (12), the real part also becomes convergent.

[19] We calculate the highly oscillating integral, Eq. (12), by using the QUADPACK FORTRAN package [20].

[20] http://www.netlib.org/quadpack/.

[21] A. Aktas *et al.* (H1 Collaboration), Eur. Phys. J. C **46**, 585 (2006).

[22] S. Chekanov *et al.* (ZEUS Collaboration), Eur. Phys. J. C **24**, 345 (2002).

[23] M. Capua *et al.*, Phys. Lett. B **645**, 161 (2007).

[24] L. Jenkovszky, V. Magas, and E. Predazzi, Eur. Phys. J. A **12**, 361 (2001).

[25] V. K. Magas, Phys. At. Nucl. **68**, 104 (2005); arXiv:hep-ph/0411335; arXiv:hep-ph/0611119.